HHS Public Access

Author manuscript

Annu Rev Biomed Eng. Author manuscript; available in PMC 2019 June 14.

Published in final edited form as:

Annu Rev Biomed Eng. 2018 June 04; 20: 301–327. doi:10.1146/annurev-bioeng-071516-044532.

From Nanoparticle Heating to Thermoregulation: A Multiscale Bioheat Transfer Review

John C. Bischof[1] and **Kenneth R. Diller**[2]

[1]Department of Mechanical Engineering, University of Minnesota, Minneapolis, Minnesota 55455

[2]Department of Biomedical Engineering, University of Texas, Austin, Texas 78712

Abstract

Over the past decade the field of bioheat transfer has grown dramatically in part due to new medical applications. Here we review a part of this growth stemming from nanoparticle heating to whole body thermoregulation. This includes foundational multiscale engineering developments and physiological expertise that support the whole field of bioheat transfer. Many of these new technologies must be considered as revolutionary rather than just evolutionary. The gateway to these advances has occurred via a combination of new engineering materials and methods that may be adapted for heat transfer applications in conjunction with remarkable mechanistic insights into the function of living systems spanning from the molecular and cellular to physiological levels. Thus, the length scales across which these bioheat transfer phenomena occur span at least six orders of magnitude. This review presents a concise summary of the current state of understanding of the engineering and physiological principles that govern these bioheat transfer processes over nm to cm scales and beyond. We then show the dramatic opportunities for translation and impact in prophylactic, preservative, diagnostic, and therapeutic applications based on nanoparticle heating and whole body thermoregulation.

Keywords

thermoregulation; thermally enhanced sleep efficiency; nanowarming; cryopreservation; thermal contrast diagnostics; nanoparticle heating

1. INTRODUCTION

The science of bioheat transfer has experienced significant advances in recent years in both its foundational technologies and in broad areas of medical impact. Synergistic developments in complementary engineering technologies and instrumentation, plus the

bischof@umn.edu.

DISCLOSURE STATEMENT

Patent applications have been submitted by Dr. Bischof and Dr. Diller that cover multiple items of IP discussed in this paper. Ownership rights to these patents reside with The University of Minnesota and The University of Texas System, respectively. Some patents are licensed to companies in which Dr. Bischof or Dr. Diller hold an equity interest. Dr. Diller has an equity position in Mercury Biomedical, LLC., a corporation that holds a license from the University of Texas for STS technology. Dr. Bischof has an equity position in Vigilant Diagnostics, LLC, a corporation that is developing thermal contrast technology. Some of the research reported herein has been funded through Mercury Biomedical. Dr. Diller has not received any direct financial compensation from Mercury Biomedical.

rapid progress in cell and molecular biology have contributed substantially to these achievements. It is quite remarkable that these advances have occurred in the context of processes that transpire across multiple length scales spanning nanoscale to cell, tissue and even whole organism, equivalent to six orders of magnitude in total. However, since its inception, the field of bioheat transfer was conceived and developed following a greatly different pathway.

Historically bioheat transfer has been focused on a diversity of problems including energy interactions between species (animal and plant) and their environments, with internal heat flow processes, particularly via convection of blood, with thermally derived injuries, and with energy-based surgical procedures, and therapeutic technologies. One of the pioneers in bioheat transfer, Alice M. Stoll, wrote a history of the field a half century ago (1). Another pioneer, John C. Chato, published multiple historical accounts a quarter century later (2; 3). In the same period Shitzer and Eberhart edited a comprehensive two volume treatise containing 28 extensive chapters on the current status of bioheat transfer (4). More recently there have been other broad-based reviews of bioheat transfer (5-7).

In this review we provide an overview of current cutting edge understanding and applications of nanoparticle heating and thermoregulation in bioheat transfer. Thus, the review is not comprehensive, but rather derived from the perspectives of the authors according to their participation in the development of multiple arenas of application.

2. NANOPARTICLE HEATING

Recent reviews highlight the use of gold (Au) and iron oxide (IO) nanoparticle heating for biomedical applications including most notably cancer thermal therapy (8-13). In addition, we have now shown the IO nanoparticles can be used to successfully warm larger 50 – 80 mL cryopreserved systems in radiofrequency fields (14). Further, laser gold nanoparticles can be heated with ms pulse or continuous wave laser irradiation for diagnostic and cryopreservation applications (15; 16). Other important work with μs and faster pulsed lasers system which selectively destroy or manipulate at the molecular and cellular level will not be reviewed here and can be found elsewhere (12; 17-19).

2.1 A primer on gold and iron oxide nanoparticle heating

Gold (Au) and iron oxide (IO) nanoparticles can be used for nanoscale and bulk heating by their careful design for optimal interaction with electromagnetic fields such as radiofrequency (RF) and light. As several embodiments of these particles have received FDA approval, this heating can be used for tumor hyperthermia and a growing number of other biomedical applications (20). These applications are usually determined by the size of the system, NP type, concentration, distribution and aggregation state to create local heat generation which we will represent here with the term specific absorption rate or SAR (W/m^3), or SAR_{NP} (W/mg NP) both measures of heat generation, as previously reported (12; 21). The conversion is simply SAR = [mg NP/ml]* SAR_{NP}.

Typical SAR_{NP} for IO and Au nanoparticles used for bulk tumor hyperthermia treatments range from 0.1 – 100s of W/mg NP given typical RF (10 kA/m and 100 kHz frequency) and

Laser (5 W/cm^2 fluence rates and 500 – 1064 nm wavelength) fields. This translates into useful volumetric SARs of 0.1 – 10s of MW/m^3 for concentrations ranging from μg/ml for Au and mg /ml for IO (21). Importantly, under these conditions nanoparticles are ineffective at heating cells or their own surfaces above ambient (i.e. only μK for RF and mK for laser possible). To achieve ≥ single K (°C) temperature rise at the nanoparticle surface the laser fluence rate needs to be increased by ≥ 3 orders of magnitude (10^4 W/cm^2) as noted in other work (21-23). After introducing the basic mechanisms and measurement of nanoparticle heating several new applications in cryopreservation and diagnostics will be reviewed.

Radiofrequency IO NP Heating.—Iron oxide nanoparticles couple with radiofrequency fields and can effectively heat bulk systems (mm – cm) (13; 24). An important advantage of IO is that typical 100's kHz radiofrequency fields can penetrate through the entire body without significant interference or attenuation (25). This allows heating of deep-tissue NP deposits for the time scales of minutes required for cancer destruction or for warming of vitrified systems (14; 26; 27).

The SAR for IO nanoparticles, is dependent on the field strength (kA/m) and frequency of the field (kHz) for RF heating of a given concentration of IO (Fe_3O_4 or Fe_2O_3) nanoparticles (24; 26). Experimentally, the rate of heat generation can be estimated from the time-dependent temperature profile of a sample subjected to heating as shown in Figure 1. The initial temperature increase is linear before the heat diffusion and losses are significant. Thus, SAR (W/m^3) can be estimated as:

$$SAR = \rho C\left(\frac{dT}{dt}\right)_{initial}$$

where ρ is density, C specific heat and dT/dt the initial rate of rise in temperature of the sample within the experimental apparatus, as previously described (26; 27).

One interesting example of how such an experimental apparatus can be used is in the characterization of different IO particle heating. Specifically, Fe_3O_4 NPs smaller than ~20 nm generally exhibit a single magnetic domain with superparamagnetic behavior, while NPs larger than 20 nm have multiple domains with ferromagnetic behavior (13; 26). Thus heating due to relaxational losses by Néelian (rotation of the magnetic moments within the NP) and Brownian (due to viscous effects as the entire NP aligns with the external magnetic field) mechanisms are present. These losses depend on NP size, concentration, magnetic properties of the nanoparticle, shape and crystalline structure, and have been theoretically described (28; 29). Numerous studies now focus on experimental work to reach the highest possible SARs for IO nanoparticles by controlling both the coating (30), crystalline content and size (31; 32) and the external radiofrequency fields (33). The heating of IO nanoparticle is generally represented as a specific absorption rate (SAR) which is W/mg Fe (26; 32). However, these idealized measurements come with caveats as work has now clearly demonstrated that the aggregation state of superparamagnetic particles in high concentration protein or salt solutions can reduce SAR by up to 50% (34-36). These effects can be mitigated by appropriate coating such as with mesoporous silica and poly-ethylene glycol (30). However, this underscores that heating generally requires IO NP concentrations ≥ 1

mg/mL for heat based treatment of cancer (26; 37), and for rewarming vitrified systems (14). In the case of cancer this is a difficult concentration to reach by intravenous injection followed by passive biodistribution, thereby necessitating interstitial injection of surrounding tissues with IO NP solutions (38; 39). It also begs the question of what the local concentration is and by what imaging technique it can be quantified. Recent exciting work with special MR pulse sequences including Sweep Imaging with Fourier Transform (SWIFT) show the ability to quantify IO nanoparticles up to 3 mg Fe/g tissue, or possibly higher, for this purpose (14; 40; 41).

Laser Au NP Heating: Alternatively, Au nanoparticles that couple plasmonically to laser light at specific wavelengths can be used to heat systems in the nm – cm scale (12; 42). Unlike RF fields, laser light typically attenuates within millimeters of the surface of a system although near infrared wavelengths (NIR) can penetrate to a cm or possibly beyond by avoiding water absorption in some systems (12). Nevertheless, Au nanoparticles are many orders of magnitude more efficient absorbers than IO using typical CW laser fluences. This means that laser gold nanoparticle heating can be used on applications that range from genetic and molecular manipulation, to endosomal drug release, protein denaturation, single cell destruction, warming of cryogenically stored embryos, and thermal therapy of cancer (12).

Lasers have been shown to interact plasmonically with gold nanoparticles at defined wavelengths to affect much more intense heating than iron oxide. For instance, when light of a given wavelength (and therefore frequency) interacts with metal particles, the electromagnetic field drives the oscillation of free electrons in the metal. The frequency of light and electron oscillation converge at the surface plasmon resonance (SPR) where a maximum interaction occurs. This energy can then be transferred to the metal particle either by absorption, which ultimately becomes heat, or it can be re-emitted at the same frequency (Rayleigh scattering) or at a shifted frequency (Raman scattering) (43; 44). SPR leads to higher absorption and scattering with Au NPs as compared with traditional light interaction with dyes (45).

Since the optical properties of Au NPs are important for heating applications, accurate methods to measure and predict them are needed. The measure of absorption and scattering is typically given as C_{abs} and C_{sca}, the absorption and scattering cross section respectively. The sum of these is C_{ext} the extinction cross-section which is what can be directly measured in a UV VIS spectrophotometer in the lab. Unfortunately, deconstructing C_{abs} and C_{sca} from C_{ext} requires further work. We have proposed to address this through temperature measurement on the bulk level. For instance, the SAR is based on laser fluence rate (I – W/m^2) interacting with a concentration of N ($\#/m^3$) of NPs with specific absorption cross sections (C_{abs} – nm^2) during heating to create the heat generation:

$$SAR = N C_{abs} I \quad (1)$$

This SAR (W/m^3) can again be related SAR_{NP} (W/mg NP) by multiplying by the NP concentration as mentioned above. SAR is accessible experimentally by interrogating the

inlet and outlet power of the laser after passing through the sample. This is shown as $P_{in} - P_{out}$ which upon manipulation can be directly related to the power dissipated in a single nanoparticle, P_{GNP} as shown in Figure 2. Furthermore, C_{abs} (and C_{ext}) can be estimated by Discrete Dipole Approximation (DDA), and compared to experimental bulk heating measurements as a function of particle polydispersity and fluence (46). Thus, the experiment in Fig. 2 allows a comparison between the theoretically predicted nanoscale heating (C_{abs} I) and the actual bulk heating to reconcile the true value of C_{abs} as a constant or variable (i.e. polydispersity) within the system. Recently, this approach was used to assess the heating of gold nanoparticles and rods and found that spherical C_{abs} is not much changed by polydispersity, but C_{abs} changes dramatically due to polydispersity in rods and can diminish the expected bulk SAR by up to 70% (46). Further studies using this approach to estimate SAR reduction (or increase), due to aggregation are planned.

For most applications, a temperature rise ≥ °C within the bulk system is desireable. For instance, the expression for temperature increase over the environment at the center of a uniformly heated spherical volume at steady state is (21; 47):

$$\Delta T = \frac{R^2 SAR}{2k} \quad (2)$$

Assuming all SAR is generating by nanoparticles within this volume of radius R, the temperature rise at the periphery over the temperature far from the sphere can be obtained by:

$$\Delta T = \frac{R^2 SAR}{3k} \quad (8)$$

For thermal therapy, we might assume the system to be a spherical tumor that needs to be heated by 10 °C and calculate the SAR (neglecting perfusion) that would achieve this:

$$SAR = \frac{3k \cdot \Delta T(r = R)}{R^2} = \frac{3k \cdot 10[\,^{\circ}\mathrm{C}]}{R^2} \quad (3)$$

The inverse dependence on the square of radius is of great significance and indicates why it is difficult to heat at the nano and microscale with nanoparticles. Specifically, as the radius of the heated region drops the SAR (W/m^3) must increase dramatically. Thus, radiofrequency heating of IO is really only feasible in > mm^3 volumes with mg Fe/ml concentrations (26). Similar heating can be achieved with W/cm^2 laser fluence rates and three orders of magnitude lower concentrations (i.e. μg Au/ml). These ideas have already been applied to thermal therapy of tumors with perfusion using computational approaches (48; 49). Here we expand the applications for nanoparticle heating into tissue cryopreservation, diagnostics, and fish embryo rewarming (15; 16; 27).

2.2 Radiofrequency iron oxide nanowarming for tissue cryopreservation

We have recently demonstrated that IO nanowarming can be used in regenerative medicine to improve tissue and hopefully one day organ banking as shown in Figure 3. A major goal of regenerative medicine is to provide tissue and organ transplants to patients suffering from organ failure or tissue disease on an as needed basis. To achieve this, a source of banked tissues and organs is needed. Cryopreservation of tissues and storage at low temperatures provides a potential solution to this problem, with the aid of concentrated cryoprotectant formulations (6 – 8 M), viable tissues can be cryogenically stabilized in the vitreous (i.e. “glassy” or “amorphous”) state without ice crystals at vapor phase nitrogen temperatures (−160 °C) for indefinite time periods (50-53). Indeed, technology to successfully vitrify whole mammalian (rabbit) kidneys in roughly 80 mL vessels does exist (53; 54). Unfortunately, rewarming these kidneys or other bulk vitrified biomaterials from liquid nitrogen temperatures continues to be an engineering challenge as the warming rates needed to avoid devitrification (or crystallization during the warming) are typically an order of magnitude higher than the critical cooling rates to avoid crystallization during cooling (27; 54; 55). For instance, in VS55, a commonly used vitrification solution, the critical cooling rate to achieve vitrification is 5 °C/min which is achievable as already noted, but the critical warming rates of 55 °C/min needed to avoid devitrification requires nanowarming to achieve (14; 27).

Importantly, these rates need to also be sufficiently uniform throughout the material to avoid large thermal gradients. Specifically, temperature non-uniformity produces thermal stresses, which in turn may drive fracture or cracks within the tissue if they exceed the strength of the material (tensile strength of vitrified VS55 is 3.2MPa) (56; 57). A benefit of nanowarming is that the RF fields penetrate with negligible attenuation in comparison to laser, microwave or other electromagnetic fields. Thus, they can be used to couple specifically to uniformly loaded iron oxide nanoparticle concentrations. This in turn can allow uniform warming of larger systems. First we demonstrated proof of principle radiofrequency (RF) heating of biologically compatible IO magnetic nanoparticles within 1 mL (1 cm diameter) systems within a 1 kW RF system (26; 30). More recently, we were able to physically scale up nanowarming to 80 mL (5 cm diameter) systems in a larger 15 kW inductive heating coil capable of 20-60 kA/m at a frequency range of 150-400 kHz, and a resulting SARs of up to several MW/m^3 in an iron oxide nanoparticle loaded vitrified system. Importantly, further work to select or design the highest heating iron oxide nanoparticles for nanowarming is underway with the design of higher heating cores (32), and the use of higher fields (up to 60 kA/m and higher) in larger 15 – 150 kW RF systems (33). This is important since SAR is proportional to the square of the field strength so that a 3 fold increase in field from 20 – 60 kA/m should yield a dramatic improvement in SAR and the corresponding warming rates achievable. So far we have been able to demonstrate that nanowarming can match or exceed traditional convective rewarming of small 1 mL vitrified tissues, and appears to be fully scalable to 80 mL where convective warming is insufficient to quickly and uniformly warm the samples (14). Future work on nanoparticle loaded tissues and organs is currently underway to more fully probe the promise of this exciting new technology for regenerative medicine tissue and organ banking.

2.3 Thermal Contrast Diagnostics

Thermal contrast uses laser gold nanoparticle heating to improve a simple diagnostic assay called the lateral flow assay (LFA) (Figure 4). More specifically, the approach is used to increase sensitivity, quantify antigen burden, and add dynamic range to LFA diagnostics (15; 58).

Lateral flow assays are an ideal point-of-care (POC) biomolecular diagnostic device for both high-income and resource-limited settings (59-62). The LFA is cheap, fast and easy to use, making it common in medicine and home applications such as pregnancy testing (63). Unfortunately, the LFA is generally not quantitative and has low sensitivity to antigen detection in the μM to μM range (ng/mL to mg/mL) which is roughly three orders of magnitude less sensitive than laboratory based techniques (ELISA, PCR, etc.) by (63; 64). Nevertheless, there is an increasing need for highly sensitive molecular diagnostics with nM to pM detection sensitivity for protein analysis for point-of-care diagnostic devices (61). While many emerging technologies are being developed for this purpose (quantum dot bio bar codes, PCR and microfluidics, etc.) modifying or improving the LFA is also an attractive and potentially less expensive approach. For instance, we have achieved LFA improvement through laser gold nanoparticle heating, which creates a measurable temperature change when gold nanoparticles are present on the test line of the LFA (See Figure 4). This in turn improves the detection, quantification and expands the range of testing for the captured protein or analyte of interest.

With most existing gold nanoparticle (GNP) based LFAs, antibody-coated GNPs move within a nitrocellulose membrane through capillary action after the strip has been dipped in a clinical specimen. When present the target analyte binds to antibody-coated GNPs in flow. This bound complex stops wicking up the membrane when the captured antibody on the membrane recognizes the antigen-antibody-GNP complex. This leads to accumulation of GNPs at the test line of the LFA, creating a visually positive test result, shown in Figure 4 B. GNPs work well in LFA designs (Figure 4 C) because their size (10s of nm) can be designed to easily migrate through the many micron sized pores of the nitrocellulose membrane and GNPs can be easily coated with antibodies. Further, GNPs can be designed to heat under specific wavelength laser irradiation due to plasmonics, and the amount of heat generated by GNPs can be described as previously noted in Eqn. (1)

Thus, GNPs absorb laser light and generate heat in proportion to their number, and therefore bound analyte present in a diagnostic assay (12). The resulting heating is a *quantitative* measurement of antigen bound to the GNPs as shown in Figure 4A (12). Importantly, this can be incorporated into a portable stand-alone reader device for POC diagnostics (58). Figure 4B demonstrates the value of this approach on a visually negative sample (S2) which is actually positive by thermal contrast (15). This concept can be generalized to a population being tested for Strep throat or Flu where increasing the sensitivity can help reduce false negatives without waiting for laboratory testing, thereby allowing patients faster treatment and a reduction in infectious transmission to the general population. In the reader, the laser excites the nanoparticles and the IR camera or detector measures the rate of heating and the end-point temperature rise in the LFA after laser exposure. While the data shown is a dilution study of a patient sample, a follow on study was able to also show benefit in a

clinical cohort study of Cryptococcus (65). The reader was then tested on malaria, C. difficile and flu demonstrating 8 fold increase in threshold detection values without any modification of the existing commercial LFA (58).

While this is an encouraging result, LFAs are still orders of magnitude less sensitive and quantitative than laboratory based approaches. Thus, work is now focused on redesigning LFAs to function with the reader to achieve laboratory levels of detection and quantification while maintaining the speed, simplicity and low cost of the LFA. This goal appears within grasp as the absorption cross section of GNPs can be improved 10 - 100x by careful selection of wavelength and GNP design. Furthermore, the background absorption of the LFA membrane backing can be replaced by transparent material allowing a 10 × increase in laser fluence (i.e. the backing material will not overheat). This suggests that new thermal contrast LFAs may yield up to a 1000 fold improvement in detection. This would allow LFA analyte detection to move from the existing range (μM to μM) to the desired range (nM to pM) competitive with existing laboratory techniques thereby benefiting numerous diagnostics at the POC in both the developing and first world (15; 61).

2.4 Laser gold nanowarming for fish embryo cryopreservation

Laser gold nanorod heating has recently also been used to improve cryopreservation of fish embryos (16). This area is of increasing importance as in the past decade, laboratories around the world have produced tens of thousands of mutant, transgenic, and wild-type zebrafish (*Danio rerio*) lines for a wide range of vertebrate genetics and biomedical research. Maintaining all of these valuable genotypes is expensive, risky, and beyond the capacity of even the largest stock centers. Moreover, the difficulty and expense of transporting live zebrafish colonies makes multi-institutional research on zebrafish rare. In addition to the need to bank research materials, there are increasing needs to preserve the biodiversity of dwindling aquatic and other species world-wide (66). To date, zebrafish sperm have been successfully cryopreserved, but zebrafish embryos have not.

There are many barriers to successful zebrafish embryo cryopreservation (67-70), with perhaps the main issue being it's large volume (800 μ diameter). Nevertheless, both mouse oocytes (80 μm) and zebrafish embryos can reach a cryogenically stable state in liquid nitrogen by using ultra-fast cooling at roughly 90,000 °C/min with a Cryotop™ system (71; 72). To achieve this process both oocytes and embryos need to be loaded with roughly 2 M cryoprotective agents (i.e. propylene glycol, a biologically compatible anti-freeze). While the smaller oocytes can be passively loaded prior to cooling, zebrafish embryos at 1000 times the volume of the oocyte and low permeability membranes cannot. Thus, micro-injection of CPAs into the zebrafish embryo has been used followed by rapid convective cooling to achieve a cryogenically stable state.

Unfortunately, even though the fish embryo is presumed stable and viable, it has never been successfully rewarmed from this state. In short, convective warming is too slow and has consistently led to failure. Recently, however, new work has now shown that much faster rates of warming can be achieved using laser heating of india ink. This has led to dramatic recovery of vitrified mammalian oocytes when the ink is deployed around the 80 – 100 μm oocytes (71; 72). Unfortunately, extracellular deployment of the absorber fails upon laser

warming with zebrafish embryos. We recently reported the first limited success by injecting biologically compatible gold nanorods instead of india ink, which was found to be toxic, within the larger zebrafish embryo. As micro-injection of CPA is already used, we were able to add 2 pM plasmonically active gold rods (1064 nm resonant) both into the embryo and surrounding it. This allowed the cryogenically stable embryo to be both warmed from a 1064 nm laser pulse (~1 ms) that heats the GNRs and surrounding embryo as shown in Fig. 5.

The projected rate of warming of 1.4×10^7 °C/min effectively outruns any ice growth yielding 30% viable and developing embryos. While the viability drops to just 10% over 24 hr and no survival has been recorded beyond 3 days, this is still promising in comparison to 0% viability, structure, or movement at all time points in convectively warmed controls. Further work investigating laser absorbers with pulse time and laser fluence rate are under way to optimize this approach. With further improvement these results suggest the potential in the future to bank embryos of zebrafish, an important biomedical vertebrate model system, transform the maintenance of genetic diversity of other fish while establishing a platform technology for germplasm banking of other vertebrate and non-vertebrate species.

3. MACRO - BODY CORE TEMPERATURE MANIPULATION

In comparison to the new fields of BHT at the nano and micro scales, macro scale studies go back to the beginning of the discipline and constitute the primary legacy. Although macro scale bioheat transfer has been explored actively for centuries, it is interesting that in recent times there have been major innovations and advances with the potential for significant health benefits. Many are driven by therapeutic needs, but it is interesting that some heat transfer methods have demonstrated health prophylaxis. For example, heat and cold have been used therapeutically to enhance the healing of injured soft tissues for centuries and even millennia (73). Nonetheless, advances in understanding the physiological response to heat and cold has facilitated more effective and lower risk technologies (74-77). Likewise, energy based surgery methods have continued to evolve in diverse directions, supported by innovations in devices and instrumentation (78; 79). Unfortunately, space limitations do not permit any of these advances to be discussed in detail. Rather, a recent totally unanticipated discovery by the second author will be presented. Although the technology and its clinical translation are still in the emerging stages, the story illustrates that there remain opportunities for combining innovations in engineering and physiological understanding of bioheat transfer to produce new therapeutic methods.

3.1. Thermoregulatory Control Mechanisms

At the whole body scale there have been important breakthroughs in understanding physiological functions that govern heat transfer processes. One area of interest deals with how the body moves heat between the core and periphery so that it may be exchanged with the local environment. Although it has long been known that blood flow to the arteriovenous anastomoses (AVAs) in glabrous skin (glabrous skin blood flow – GSBF) of the palms and soles constitutes the primary heat transfer portal between the body core and the environment (80-82), this access has generally only been available under special conditions of heat stress

or surgical procedures with general anesthesia that result in a state of AVA vasodilatation. The mechanisms that control blood flow for regulatory heat transfer have been studied extensively (83), and it is clear that there are unique, differential processes that govern convective blood flows to the glabrous and nonglabrous regions. The preoptic anterior hypothalamus (POAH) is clearly the key control component, it is thought that other control centers may also be involved (81; 83; 84).

We have recently discovered that simple and safe heating on selected areas of the skin surface can open the AVA flow on demand, thereby creating a convenient and effective pathway to induce heat flow between the body core and environment. Upregulation of AVA flow is produced by mild heating superficial to the spinal cord, particularly in the cervical region. The method is called selective thermal stimulation (STS) in which a small amount of energy is input to a very localized volume of control tissue to produce a much larger overall thermoregulatory effect (85; 86). This technology can be applied to develop a new generation of therapeutic devices based on having proactive access to control of thermoregulation processes.

3.2. Selective Thermal Stimulation in Animals

The existence of an extracerebral thermoregulation control function associated with the spine has been recognized for more than 100 years (87). Manipulation of the spinal cord temperature as a means of controlling body temperature has been practiced more than 50 years (88), including demonstration experiments in more than a dozen mammalian and avian species that maintain a constant core temperature, including the ox (89), goat (90), sheep (91; 92), dog (93-95), pig (96), cat (97), guinea pig (98), rat (99), monkey (100), rabbit (101; 102), pigeon (103), penguin (104), and goose (105). Virtually all of these foregoing experiments were conducted using a highly invasive procedure in which water circulation tubing was implanted along the length of the spine through or around the vertebral canal and, sometimes, also surrounding the hypothalamus. Water was circulated at regulated temperatures to establish the temperatures of the spinal cord and hypothalamus independently. For example, in dogs (93-95), separate individual warming of the hypothalamus and of the spine both caused animals to upregulate their endogenous heat rejection processes. This response presumably occurs because key thermosensory tissues are made locally warmer than the body in general, eliciting a response to reject heat, even though the region of over-heating is limited to the spine or hypothalamus. When both warming stimulations were applied simultaneously, the effect was additive, beyond what could be achieved by either hypothalamic or spinal control individually (94). The threshold core temperatures were reduced from normal conditions for which heat rejection mechanisms are invoked. Further, individual and simultaneous cooling of the spine and hypothalamus produced the same type of results. The magnitude of metabolic upregulation due to shivering was greater of simultaneous cooling stimuli than for cooling either the spine or hypothalamus individually (94).

Perhaps one of the most impressive demonstrations of this phenomenon was developed using oxen as a model subject (89). A 234 kg Ox had ten U-shaped polyethylene water flow tubes inserted into the peridural space of the vertebral canal spaced from the lower lumbar to

the upper cervical region six weeks prior to experimentation. The animals were placed into a (very large) calorimeter to measure heat transfer with their environment during spinal heating during a series of 9 trials at serially higher stimulation temperatures covering the range from 40°C to 47°C. For heating periods as long as six hours the subjects rejected heat to the environment at a rate greater than their basal metabolism and that was in proportion to the heating temperature. Thus, the core temperature measured at the external meatus dropped (from the thermoneutral value of about 38.5°C) until a new equilibrium state was reached, although for the strongest stimulations, the core temperature was still falling after six hours at 33°C. The rate of stimulation heat input was easily measured from the flow rate and temperature change of water as it passed through the tubing, and the rate of heat rejection was obtained directly from the calorimeter. For all trials, during the first hour of heating, the gain for the process defined as the ratio of rate of heat rejection to rate of stimulation heat input was approximately 8:1. Although only a very localized region of thermoregulatory tissue along the spine was being heated, the animal's response was to reject eight times as much body heat to the environment. In a somewhat complementary experiment microwave heating of the hypothalamus of goats (106) resulted in a 10°C core temperature drop, pointing to the parallel thermoregulatory control functions in the hypothalamus and spine.

Although there exists data from many labs that document the combined control of effects of the hypothalamus and spinal cord on thermoregulation, the mechanism this interaction has not yet been fully clarified. Some researchers have characterized the effect as additive (94; 95) and others as multiplicative (107). Most importantly, although many years have passed since the foregoing early animal experiments, this phenomenon remains to be characterized in humans.

3.3. Selective Thermal Stimulation in Humans

The implications of adaptation of selective thermal stimulation (STS) in humans for translation to therapeutic devices is significant. Hypothalamic control over thermoregulation is endogenous and is continuously operational except for special circumstances such as anesthesia (108). The human hypothalamic controller is constantly engaged and is responsive to dynamic alterations in a person's physiological state, the level and nature of physical activity, and to environmental thermal loading, be it cooling, neutral, or heating. It directs physiological thermal function within performance boundaries that are well understood. However, if STS acts additively to the hypothalamus, or just augments the native strength of the process of convective heat flow between the body core and surface, there may be circumstances in which thermoregulatory function may be boosted by activation of STS for therapeutic benefit. One can either lower or raise the core temperature by a two step process of first using STS to enhance AVA blood flow, and second, applying heat exchangers to the glabrous skin surfaces to add or remove heat from the blood before it returns to the core. This approach can extend the magnitude of operation of thermoregulatory processes, providing access to therapeutic states not otherwise available. Heller and Grahn have developed an alternate mechanical means of upregulating glabrous skin blood flow based on exposing distal limbs to a negative pressure to distend AVAs for which substantial blood flow is already established (80; 109-111). Presumably, because sympathetic vasoconstriction

is invoked via an upstream neurological flow sphincter, it is not possible to mechanically distend an AVA that is not already actively flowing.

It is intriguing that although the power of STS in directing thermoregulatory process has long since been demonstrated in numerous mammalian and avian species, it appears that there has never been a translation to humans, even though implications for adaptation in therapeutic processes is very attractive. However, we have now implemented and measured the STS phenomenon in hundreds of human trials. A large number of these trials were exploratory to characterize STS after it was first realized in humans. A typical physiological response is shown in Figure 6 for which GSBF was monitored via a laser Doppler flow probe mounted to the finger pad. A short initial period is used to establish baseline perfusion for the subject, following which STS is alternately applied and withdrawn via a heating pad applied on the cervical area. The GSBF follows STS upward and downward with a time delay, in this case, of about 5 to 10 minutes. Mechanistically, part of this delay is associated with the diffusion of heat between the skin surface and deeper sensory tissues, but that is generally no more than a few minutes, depending on anatomical variables such as thickness of the subcutaneous fat layer. Other contributing factors may include the temporal functioning of the control network, that may vary substantially among individuals, and the current dynamic status of thermoregulatory control. This latter factor is complex and nonlinear. It has been described as a thermoregulatory momentum relating to the magnitude and direction of AVA vasoactivity (85), although the mechanism has not been identified.

A complementary study is in process to assess STS from an alternative perspective. This study is based on classic foregoing studies by Sessler and colleagues on the influence of anesthesia on thermoregulatory control in humans. Figure 7 presents data for the effect of one anesthetic agent, desflurane (112), that acts consistently with other anesthetics (112-117). Subjects participated in a randomized cross-over trial in which they were cooled from a thermoneutral state of minimum AVA vasoconstriction achieved by a combination of warming the core and mean skin temperature. With the mean skin temperature held constant by a water perfusion suit, the core temperature was lowered by central venous infusion of cold lactated Ringer’s solution. The thresholds for onset and completion of AVA vasoconstriction were noted, followed by the threshold for shivering. Anesthesia substantially lowered the temperature at which vasoconstriction initiated, meaning that high levels of GSBF were maintained at core temperatures far lower than normal, leading to the hypothermia that occurs during surgery (perioperative hypothermia). All anesthetic modifications of thermoregulation were dose dependent (108).

Our STS experiments were designed with the same perspective (based on advice from the Sessler group) to determine whether STS would significantly lower the threshold temperature for vasoconstriction onset. If so, then by applying heat exchangers onto the glabrous skin surfaces (palms and soles), it is possible to manipulate the heat flow into and out of the core under physiological conditions not otherwise available. Although the full trials are not yet complete, Figure 8 shows exemplar control and STS data for a subject cooled from a state for which vasoconstriction initially was minimized by warming the mean skin temperature with a water perfused suit. This data illustrates that STS does indeed lower the threshold temperature by about 0.5°C for the onset of vasoconstriction during cooling

from the thermoneutral state thereby creating a substantial window of opportunity to effect high level convective heat transfer via blood flow to the core that would not be available without STS. A second feature of the data is that the precooling level of GSBF is higher with STS than during control when it was maximized only by manipulation of mean skin temperature. The implication is that the combined effects of mean skin and core temperatures plus STS on GSBF appears to be greater than of either individually. Although these results are not yet fully documented, they align with the past experiments on mammalian and avian species by Jessen and others (88). Further data relating to this phenomenon is presented in the following section. A major advantage of STS is that opens the opportunity to proactively and effectively manipulate the body core temperature for diverse medical purposes, some involving cooling and some heating. Further, apart from heat transfer effects, vasodilating the AVAs alters the peripheral vascular resistance of the cardiovascular system, which also has multiple substantial implications for health and well-being.

4.4. Therapeutic and Prophylactic Applications of STS

Three applications of STS will be discussed briefly: one for adjusting the core temperature upwards; one for adjusting the core temperature downwards; and one for depressing the action of vasoconstriction on AVAs to achieve a higher level of GSBF. The first two involve applying either cooling or warming heat exchanges to the palms and soles in conjunction with having GSBF upregulated by STS. The latter simply uses native heat exchange with environmental air during sleep.

Warming the body core is of critical clinical importance during surgical procedures under general anesthesia. Perioperative hypothermia of even 1°C may lead to an array of adverse, serious complications (118) such as bleeding disorders (119), increased surgical site infections (120), extended hospitalization (121; 122), and morbid cardiac events (123). Consequently, the standard of care during surgery under anesthesia is to use some form of warming to defend against the occurrence of perioperative hypothermia. By far the most widely adopted method is via forced air heated blankets of which there are multiple alternatives (124), although alternative methods exist such as circulating water garments (125) and solid state resistance heaters (126). Given the relatively poor convection properties of air, it is not surprising that the alternatives out perform it thermally, although the relative performance remains a somewhat controversial issue (127; 128). A recent study of more than fifty-eight thousand patients who underwent surgeries lasting more than an hour and who received forced air warming showed that about 2/3 experienced a core temperature drop below the target value of 36°C at some time during their procedure (129). Clearly, there is an opportunity for improved thermal performance of these perioperative warming devices. Plus, there is accumulating, though still equivocal, data that the exhaust flow from forced air warming may entrain bacterial contaminants and introduce them into the surgical site, especially during total joint replacement procedures (130-133).

STS offers a potentially advantageous alternative to existing technologies for core temperature manipulation. Although anesthesia previously has been thought to fully vasodilate AVAs, which is does in the absence of an independent stimulation that acts

additively, a recent preliminary clinical trial on a diverse group of twelve patients during surgery resulted in an average additional increase of 40% in GSBF above the level established during a hour or more of prior anesthesia. The implication is that STS in conjunction with heating the palms and soles will be more effective in maintaining core temperature by using the body's natural heat transfer pathway than is heating applied over large areas of nonglabrous skin by circulating air, water or other means. In addition, the application of heating pads to the palms and soles blocks the primary site of heat leak from the core during anesthesia when other warming means are used, and provides much better access to the body surface during surgery. Further clinical studies are currently in progress to measure the ability of STS in combination with glabrous skin heating to warm the body core in anesthetized subjects.

In a second parallel study, STS is applied in conjunction with mild cooling of glabrous skin surfaces to lower the body core temperature on demand. Key application areas include providing therapeutic hypothermia in response to medical events that cause major organ ischemia, especially of the brain. These encompass cardiac arrest, stroke, and traumatic brain injury, among many others. Lowering the core temperature presents a striking physiological challenge since the body has effective defense mechanisms to guard against any significant drop in its internal temperature. As noted earlier, these thermoregulatory processes are invoked with a tight control bandwidth of just a few tenths °C. Since therapeutic hypothermia has been demonstrated to reduce morbidity and mortality when it can be applied in a timely and effective manner, there is a great incentive to develop methods and devices to use it clinically. A diverse collection of approaches are in practice that use processes such as: to apply intense cooling over a large portion of the body surface to overwhelm the ability of the thermoregulatory system to defend itself; to invasively introduce cold fluids intravenously or via lavage to thermally dilute the energy stored in the core; and/or to apply pharmacological agents to immobilize thermoregulatory function. All of these approaches have inherent disadvantages, not the least of which is that they are most judiciously applied only within a medical facility and require trained personnel. Since the tissue deterioration process begins with ischemia induction, it is of advantage to be able to start hypothermia as soon as possible, most desirably within the first 90 or so minutes when the "critical window of opportunity" exists for low temperatures to reverse ischemic damage.

STS based devices and methods offer a unique alternative to resolving all of the foregoing limitations. An STS source for cervical heating can have a light weight and small footprint for convenient storage, is totally noninvasive, and can be applied immediately in the field without the need for advanced training. Calibrated chemical cooling sources can be applied as heat exchangers to the glabrous skin surfaces. It is important that the cooling temperature not be too low in order to avoid locally induced vasoconstriction that would obviate convective heat transport with blood (134). By lowering the effective core temperature for AVA vasoconstriction, STS provides an opportunity to safely and effectively remove energy from the body by endogenous mechanisms that minimize collateral stress applied during the process. This approach is parallel to that applied many decades previously by Jessen and colleagues to induce oxen to reject copious amounts of internal heat to lower their core temperatures (89). Initial testing indicates that cooling rates from human subjects on the order of 140W are possible and that these should be clinically significant (85).

A third arena of use for STS is to enhance the onset and quality of sleep. Long-standing research in thermal physiology has documented that the human thermoregulatory system operates on a circadian cycle in coordination with sleep (135; 136). The thermoregulatory cycle is functionally involved in driving the sleep-onset process (137), although the inverse is not true (138). GSBF plays a key role in governing sleep performance. Krauchi has shown how modulation of blood flow to AVAs in glabrous skin of the hands and feet plays a major role in determining sleep quality. Vasodilated AVAs (warm hands and feet) promote rapid sleep onset (139), whereas vasoconstricted AVAs produce delayed sleep onset (140).

Physiological sleep data show that as late hours in the circadian cycle approach, there is a significant upregulation in GSBF, opening the primary heat exchange portal from the warmer core to the (usually) cooler environment. A subsequent drop in core temperature occurs via enhanced convection of blood to glabrous skin, facilitating the loss of core heat to the environment, with a time constant on the order of 2-3 h, and with sleep onset following thereafter in an additional 0.5 h (141). Another important benefit of AVA vasodilation during sleep is that the diminished terminal vascular resistance to blood flow results in a reduced sleep-time blood pressure that is increasingly recognized as protective against risk of cardiovascular diseases and major organ (kidney, eye, etc.) pathology (142; 143). An overnight dip in blood pressure has been identified as a significant contributing factor in lowering the occurrence of cardiovascular derived events by as much as 1/3 or more, even when daytime blood pressure is elevated - hypertensive (144). The National Sleep Foundation (145) has identified that one or more symptoms of insomnia, including prolonged delay in sleep onset, poor sleep continuance, waking too early, and feeling unrefreshed in the morning, are experienced by an estimated 50% of the US adult population at least a few nights per week, often compromising daytime performance and increasing the risk of experiencing driving, home, and workplace accidents (146; 147). Absence of the normal nocturnal decline in core temperature by about 1°C can be associated with sleep-onset insomnia (148). Common causes of abnormally high nighttime temperature are improper HVAC environment, circadian rhythm dysregulation (e.g., jet lag, shift work), and thermoregulatory dysfunction. The latter condition may occur at any time of year and is thought to affect tens of millions of US citizens. Typical accommodation is attempted by downward adjustment of the air temperature in the sleep room, with targets as low as 60°F to 68°F (15.6°C to 20°C), quite often to the discomfort and consternation of the sleeping partner.

In view of the foregoing information, it is clearly anticipated that STS may be efficacious for enhancing sleep onset and quality and for facilitating a transient drop in overnight blood pressure by suppressing vasoconstriction of AVA flow. STS may be applied shortly prior to the desired time of sleep onset with a defined set of physiological responses: distal AVAs will be vasodilated (i.e., vasoconstriction suppressed) resulting in warming of hands and feet; core heat loss via GSBF will increase, precipitating an early initiation to the overnight core temperature drop; and the desired dip in blood pressure will begin early in the sleep cycle, providing an extended period of overnight cardiovascular recovery.

Figure 9 shows overnight physiological data for a sleeper with and without the use of STS for a brief period at bed time. This data illustrates the efficacy of STS relating to sleep

function for a subject who typically experiences difficulties in falling to sleep after going to bed. The data starts with a 20 min baseline period prior to STS. Plot (a) illustrates blood flow to glabrous skin on the sole of the foot as monitored with a laser Doppler flow meter. In the control trial without STS the blood flow is in continuous decline for more than 3 hours, associated with difficulties in sleep onset. With STS applied, blood flow to the feet is initiated early in the sleep cycle and rises rapidly to a maximum value that is maintained through the night. (b) presents data for surface temperature on the foot sole. Both the control and STS trials directly reflect the levels of GSBF. Warm feet are consistent with a 3X average shorter period required for sleep onset (139). (c) shows overnight core temperature values. A significant drop in core temperature is required for a quality sleep experience (135; 149; 150), and heat transfer from glabrous skin with a high blood perfusion rate is the key to eliminating heat from the body core. With the upregulation in GSBF produced by STS, core body temperature drops immediately and continuously to the overnight nadir. In contrast, for the control trial core body temperature remained elevated at a high level for several hours before an eventual fall. The time lag of nearly fours hours most likely represents a loss in restorative sleep potential through the night. (d) shows the continuously monitored mean arterial pressure. Longitudinal studies have documented long term health benefits from an extended significant dip during sleep (143). With early STS induced vasodilation of large bore AVAs (about ten times the diameter of capillaries), the cardiovascular resistance against which the heart must pump is reduced, thereby allowing a depressurizing of the system overnight. In contrast, in the absence of STS at the start of the overnight cycle, the MAP remains elevated for hours before eventually dropping.

Implementation of STS into the sleep environment can be minimally obtrusive and may be a valuable technology to increase sleep performance. For people who suffer from insomnia associated with thermoregulatory dysfunction, STS can provide a direct method for relief. For people who are “normal” sleepers, it is likely to still lead to an improved sleep experience and daytime function.

5. CONCLUDING THOUGHTS

Bioheat transfer offers a research platform rich in opportunities for applying engineering principles to the design and development of important new medical devices and methods. The pathways are diverse, with many remaining to be discovered. This review shows examples that cover many orders of magnitude in length scales from nano to physiological and from technology bases from long established thermoregulation to state-of-the-art nanoparticle heating. By no means is the material coverage comprehensive. There is every reason to believe that the future holds new discoveries that will contribute substantially to be betterment of medicine and society.

ACKNOLWEDGEMENTS

Dr. Diller’s research has been sponsored most recently by National Science Foundation Grant CBET 1250659 and National Institutes of Health Grants R01 EB015522 and R41 GM119841, and the Robert and Prudie Leibrock Professorship in Engineering at the University of Texas at Austin. Dr. Bischof’s research has been funded by NSF 1066343, NSF 1336659, R43HL123317, R41 OD024430-01 and DOD W81XWH-15-C-0173, DOD W81XWH-16C-0074, DOD W81XWH-16-1-0508 an Institute for Engineering in Medicine Seed Grant, a

University of Minnesota MN Futures Grant, NIH CTSI Seed Grant, a UM / Mayo Partnership Grant on Thermal Contrast and the Kuhrmeyer Chair in the Department of Mechanical Engineering at the University of Minnesota.

ACRONYMS AND DEFINITIONS

AVAs	Arteriovenous Anastomoses are shunt vessels between arterioles and venules that can vasoregulate to large diameters that accommodate high blood flow rates and convective heat transport.
BHT	Bioheat Transfer involves the generation and transport of heat in conjunction with the broad array of processes that are required to sustain life. Compared with the more general field of heat transfer, bioheat transfer is characterized by systems and materials that are more likely to be anisotropic, heterogeneous, have complex geometries, and are often regulated by highly nonlinear feedback control.
GSBF	Glabrous Skin Blood Flow is circulation of blood through AVAs for high performance thermoregulatory heat exchange.
STS	Selective Thermal Stimulation is the application of mild heating to peripheral thermoregulatory tissue, especially along the cervical spine, to cause upregulation of GSBF.

LITERATURE CITED

1. Stoll AM. 1967 Heat Transfer in Bioethcnology. Advances in Heat Transfer 4:65–141
2. Chato JC. 1981 ASME Centennial historical perspective Paper: Reflections on the History of Heat and Mass Transfer in Bioengineering. Journal of Biomechanical Engineering 103:97–101 [PubMed: 7024642]
3. Chato JC. 1992 A View of the History of Heat Transfer in Bioengineering. Advances in Heat Transfer 22:1–18
4. Shitzer A, Eberhart RC. 1985 Heat Transfer in Medicine and Biology: Analysis and Applications. New York: Plenum Press
5. Diller KR. 1992 Modeling of Bioheat Transfer Processes at High and Low Temperatures. Advances in Heat Transfer 22:157–357
6. Diller KR, Valvano JW, Pearce JA. 2005 Bioheat Transfer In CRC Handbook of Bechanical Engineering, 2nd Ed., ed. Kreith F, Goswami Y:4-292–4-361. Boca Raton: CRC Press. Number of 4-292 - 4-361 pp.
7. Charny CK. 1992 Mathematical Models of Bioheat Transfer. Advances in Heat Transfer 22:12–155
8. Beik J, Abed Z, Ghoreishi FS, Hosseini-Nami S, Mehrzadi S, et al. 2016 Nanotechnology in hyperthermia cancer therapy: From fundamental principles to advanced applications. Journal of controlled release : official journal of the Controlled Release Society 235:205–21 [PubMed: 27264551]
9. Zhao J, Lee P, Wallace MJ, Melancon MP. 2015 Gold Nanoparticles in Cancer Therapy: Efficacy, Biodistribution, and Toxicity. Current pharmaceutical design 21:4240–51 [PubMed: 26323426]
10. Jaque D, Martinez Maestro L, del Rosal B, Haro-Gonzalez P, Benayas A, et al. 2014 Nanoparticles for photothermal therapies. Nanoscale 6:9494–530 [PubMed: 25030381]
11. Hwang S, Nam J, Jung S, Song J, Doh H, Kim S. 2014 Gold nanoparticle-mediated photothermal therapy: current status and future perspective. Nanomedicine 9:2003–22 [PubMed: 25343350]
12. Qin Z, Bischof JC. 2012 Thermophysical and biological responses of gold nanoparticle laser heating. Chemical Society reviews 41:1191–217 [PubMed: 21947414]

13. Dutz S, Hergt R. 2013 Magnetic nanoparticle heating and heat transfer on a microscale: Basic principles, realities and physical limitations of hyperthermia for tumour therapy. International journal of hyperthermia : the official journal of European Society for Hyperthermic Oncology, North American Hyperthermia Group 29:790–800
14. Manuchehrabadi N, Gao Z, Zhang J, Ring HL, Shao Q, et al. 2017 Improved tissue cryopreservation using inductive heating of magnetic nanoparticles. Science translational medicine 9
15. Qin Z, Chan WC, Boulware DR, Akkin T, Butler EK, Bischof JC. 2012 Significantly improved analytical sensitivity of lateral flow immunoassays by using thermal contrast. Angewandte Chemie 51:4358–61 [PubMed: 22447488]
16. Khosla K, Wang Y, Hagedorn M, Qin Z, Bischof JC. 2017 Gold Nanorod Induced Warming of Cryogenically Stabilized Embryos Enhances Viability. ACS Nano
17. Kim JW, Shashkov EV, Galanzha EI, Kotagiri N, Zharov VP. 2007 Photothermal antimicrobial nanotherapy and nanodiagnostics with self-assembling carbon nanotube clusters. Lasers Surg Med 39:622–34 [PubMed: 17868103]
18. Zharov VP, Mercer KE, Galitovskaya EN, Smeltzer MS. 2006 Photothermal nanotherapeutics and nanodiagnostics for selective killing of bacteria targeted with gold nanoparticles. Biophys J 90:619–27 [PubMed: 16239330]
19. Braun GB, Pallaoro A, Wu G, Missirlis D, Zasadzinski JA, et al. 2009 Laser-Activated Gene Silencing via Gold Nanoshell- siRNA Conjugates. ACS nano 3:2007–15 [PubMed: 19527019]
20. Kim BY, Rutka JT, Chan WC. 2010 Nanomedicine. The New England journal of medicine 363:2434–43 [PubMed: 21158659]
21. Keblinski P, Cahill DG, Bodapati Aea. 2006 “Limits of localized heating by electromagnetically excited nanoparticles” Journal of Applied Physics 100:054305
22. Govorov AO, Richardson HH. 2007 Generating heat with metal nanoparticles. Nano Today 2:30–8
23. Richardson HH, Carlson MT, Tandler PJ, Hernandez P, Govorov AO. 2009 Experimental and Theoretical Studies of Light-to-Heat Conversion and Collective Heating Effects in Metal Nanoparticle Solutions. Nano Letters 9:1139–46 [PubMed: 19193041]
24. Dutz S, Hergt R. 2014 Magnetic particle hyperthermia--a promising tumour therapy? Nanotechnology 25:452001 [PubMed: 25337919]
25. Atkinson WJ, Brezovich IA, Chakraborty DP. 2007 “Usable frequencies in hyperthermia with thermal seeds,”IEEE Transactions on Biomedical Engineering 1: 70–5
26. Etheridge ML, Bischof JC. 2013 Optimizing Magnetic Nanoparticle Based Thermal Therapies Within the Physical Limits of Heating. Ann Biomed Eng 41:78–88 [PubMed: 22855120]
27. Etheridge ML, Xu Y, Rott L, Choi J, Glasmacher B, Bischof JC. 2014 RF heating of magnetic nanoparticles improves the thawing of cryopreserved biomaterials. TECHNOLOGY 2:229–42
28. Rosensweig RE. 2002 Heating magnetic fluid with alternating magnetic field. Journal of Magnetism and Magnetic Materials 252:370–4
29. Carrey J, Mehdaoui B, Respaud M. 2011 Simple models for dynamic hysteresis loop calculations of magnetic single-domain nanoparticles: Application to magnetic hyperthermia optimization. Journal of Applied Physics 109:083921
30. Hurley KR, Ring HL, Etheridge M, Zhang J, Gao Z, et al. 2016 Predictable Heating and Positive MRI Contrast from a Mesoporous Silica-Coated Iron Oxide Nanoparticle. Molecular pharmaceutics
31. Dennis CL, Jackson AJ, Borchers JA, Hoopes PJ, Strawbridge R, et al. 2009 Nearly complete regression of tumors via collective behavior of magnetic nanoparticles in hyperthermia. Nanotechnology 20:395103 [PubMed: 19726837]
32. Tong S, Quinto CA, Zhang L, Mohindra P, Bao G. 2017 Size-Dependent Heating of Magnetic Iron Oxide Nanoparticles. ACS Nano
33. Bordelon DE, Goldstein RC, Nemkov VS, Kumar A, Jackowski JK, et al. 2012 Modified Solenoid Coil That Efficiently Produces High Amplitude AC Magnetic Fields With Enhanced Uniformity for Biomedical Applications. IEEE transactions on magnetics 48:47–52 [PubMed: 25392562]

34. Jeon S, Hurley KR, Bischof JC, Haynes CL, Hogan CJ. 2016 Quantifying intra- and extracellular aggregation of iron oxide nanoparticles and its influence on specific absorption rate. Nanoscale 8:16053–64 [PubMed: 27548050]
35. Jeon S, Oberreit DR, Van Schooneveld G, Gao Z, Bischof JC, et al. 2016 Ion-Mobility-Based Quantification of Surface-Coating-Dependent Binding of Serum Albumin to Superparamagnetic Iron Oxide Nanoparticles. ACS applied materials & interfaces 8:24482–90 [PubMed: 27580340]
36. Etheridge ML, Hurley KR, Zhang J, Jeon S, Ring HL, et al. 2014 Accounting for biological aggregation in heating and imaging of magnetic nanoparticles. Technology (open access online):1–15
37. Kalambur VS, Longmire EK, Bischof JC. 2007 Cellular Level Loading and Heating of Superparamagnetic Iron Oxide Nanoparticles. Langmuir 23:12329–36 [PubMed: 17960940]
38. Thiesen B, Jordan A. 2008 Clinical applications of magnetic nanoparticles for hyperthermia. International journal of hyperthermia : the official journal of European Society for Hyperthermic Oncology, North American Hyperthermia Group 24:467–74
39. Etheridge ML, Bischof JC, Jordan A. 2013 Magnetic nanoparticles for Cancer Therapy In Physics of Thermal Therapy, ed. Moros E: Taylor and Francis. Number of.
40. Zhang J, Chamberlain R, Etheridge M, Idiyatullin D, Corum C, et al. 2014 Quantifying iron-oxide nanoparticles at high concentration based on longitudinal relaxation using a three-dimensional SWIFT Look-Locker sequence. Magnetic resonance in medicine 71:1982–8 [PubMed: 24664527]
41. Zhang J, Ring HL, Hurley KR, Shao Q, Carlson CS, et al. 2016 Quantification and biodistribution of iron oxide nanoparticles in the primary clearance organs of mice using T1 contrast for heating. Magnetic resonance in medicine
42. Hirsch LR, Stafford RJ, Bankson JA, Sershen SR, Rivera B, et al. 2003 Nanoshell-mediated near-infrared thermal therapy of tumors under magnetic resonance guidance. Proc. Natl. Acad. Sci. U.S.A. 100:13549–54 [PubMed: 14597719]
43. Jain PK, Huang X, El-Sayed IH, El-Sayad MA. 2007 Review of some interesting surface plasmon resonance-enhanced properties of noble metal nanoparticles and their applications to biosystems. Plasmonics 2:107–18
44. Modest MF. 2013 Radiative heat transfer. . Academic press
45. Hirsch LR, Gobin AM, Lowery AR, Tam F, Drezek RA, et al. 2006 Metal nanoshells. Ann. Biomed. Eng. 34:15–22 [PubMed: 16528617]
46. Qin Z, Wang Y, Randrianalisoa J, Raeesi V, Chan WC, et al. 2016 Quantitative Comparison of Photothermal Heat Generation between Gold Nanospheres and Nanorods. Scientific reports 6:29836 [PubMed: 27445172]
47. Rabin Y 2002 Is intracellular hyperthermia superior to extracellular hyperthermia in the thermal sense? International Journal of Hyperthermia 18:194–202 [PubMed: 12028637]
48. Salloum M, Ma R, Zhu L. 2008 An in-vivo experimental study of temperature elevations in animal tissue during magnetic nanoparticle hyperthermia. International journal of hyperthermia : the official journal of European Society for Hyperthermic Oncology, North American Hyperthermia Group 24:589–601
49. Manuchehrabadi N, Zhu L. 2014 Development of a computational simulation tool to design a protocol for treating prostate tumours using transurethral laser photothermal therapy. International journal of hyperthermia : the official journal of European Society for Hyperthermic Oncology, North American Hyperthermia Group 30:349–61
50. Taylor MJ, Song YC, Brock KGM. 2004 Vitrification in Tissue Preservation: New Developments In Life in the Frozen State: CRC Press. Number of.
51. Brockbank KGM, Chen Z, Greene ED, Campbell LH. 2015 Vitrification of Heart Valve Tissues In Cryopreservation and Freeze-Drying Protocols, ed. Wolkers FW, Oldenhof H:399–421. New York, NY: Springer New York. Number of 399-421 pp.
52. Song YC, Khirabadi BS, Lightfoot F, Brockbank KG, Taylor MJ. 2000 Vitreous cryopreservation maintains the function of vascular grafts. Nature biotechnology 18:296–9
53. Fahy GM, MacFarlane DR, Angell CA, Meryman HT. 1984 Vitrification as an approach to cryopreservation. Cryobiology 21:407–26 [PubMed: 6467964]

54. Fahy GM, Wowk B, Wu J, Phan J, Rasch C, et al. 2004 Cryopreservation of Organs by Vitrification: Perspectives and Recent Advances. Cryobiology 48:157–78 [PubMed: 15094092]
55. Steif PS, Palastro M, Wan CR, Baicu S, Taylor MJ, Rabin Y. 2005 Cryomacroscopy of vitrification, Part II: Experimental observations and analysis of fracture formation in vitrified VS55 and DP6. Cell preservation technology 3:184–200 [PubMed: 16900261]
56. Steif PS, Palastro MC, Rabin Y. 2007 The Effect of Temperature Gradients on Stress Development During Cryopreservation via Vitrification. Cell preservation technology 5:104–15 [PubMed: 18185851]
57. Eisenberg DP, Bischof JC, Rabin Y. 2016 Thermomechanical Stress in Cryopreservation Via Vitrification With Nanoparticle Heating as a Stress-Moderating Effect. J Biomech Eng 138
58. Wang Y, Qin Z, Boulware DR, Pritt BS, Sloan LM, et al. 2016 Thermal Contrast Amplification Reader Yielding 8-Fold Analytical Improvement for Disease Detection with Lateral Flow Assays. Analytical chemistry 88:11774–82 [PubMed: 27750420]
59. Yager P, Edwards T, Fu E, Helton K, Nelson K, et al. 2006 Microfluidic diagnostic technologies for global public health. Nature 442:412–8 [PubMed: 16871209]
60. Martinez AW, Phillips ST, Whitesides GM, Carrilho E. 2009 Diagnostics for the Developing World: Microfluidic Paper-Based Analytical Devices. Anal. Chem. 82:3–10
61. Klostranec JM, Xiang Q, Farcas GA, Lee JA, Rhee A, et al. 2007 Convergence of Quantum Dot Barcodes with Microfluidics and Signal Processing for Multiplexed High-Throughput Infectious Disease Diagnostics. Nano Lett. 7:2812–8 [PubMed: 17705551]
62. Nam J-M, Thaxton CS, Mirkin CA. 2003 Nanoparticle-Based Bio-Bar Codes for the Ultrasensitive Detection of Proteins. Science 301:1884–6 [PubMed: 14512622]
63. Posthuma-Trumpie G, Korf J, van Amerongen A. 2009 Lateral flow (immuno)assay: its strengths, weaknesses, opportunities and threats. A literature survey. Anal. Bioanal. Chem. 393:569–82 [PubMed: 18696055]
64. Liu J, Mazumdar D, Lu Y. 2006 A Simple and Sensitive “Dipstick” Test in Serum Based on Lateral Flow Separation of Aptamer-Linked Nanostructures. Ang. Chem. Int. Ed. 45:7955–9
65. Boulware DR, Rolfes MA, Rajasingham R, von Hohenberg M, Qin Z, et al. 2014 Multisite validation of cryptococcal antigen lateral flow assay and quantification by laser thermal contrast. Emerging infectious diseases 20:45–53 [PubMed: 24378231]
66. Lodge DM, Turner CR, Jerde CL, Barnes MA, Chadderton L, Egan SP, … Pfrender ME. 2012 Conservation in a cup of water: estimating biodiversity and population abundance from environmental DNA. . Molecular Ecology 21:2555–8 [PubMed: 22624944]
67. Hagedorn M, Hsu EW, Pilatus U, Wildt DE, Rall WR, Blackband SJ. 1996 Magnetic resonance microscopy and spectroscopy reveal kinetics of cryoprotectant permeation in a multicompartmental biological system. Proceedings of the National Academy of Sciences of the United States of America 93:7454–9 [PubMed: 8755494]
68. Hagedorn M, Kleinhans FW, Artemov D, Pilatus U. 1998 Characterization of a major permeability barrier in the zebrafish embryo. Biology of reproduction 59:1240–50 [PubMed: 9780333]
69. Hagedorn M, Kleinhans FW, Freitas R, Liu J, Hsu EW, et al. 1997 Water distribution and permeability of zebrafish embryos, Brachydanio rerio. The Journal of experimental zoology 278:356–71 [PubMed: 9262005]
70. Janik M, Kleinhans FW, Hagedorn M. 2000 Overcoming a permeability barrier by microinjecting cryoprotectants into zebrafish embryos (Brachydanio rerio). Cryobiology 41:25–34 [PubMed: 11017758]
71. Jin B, Kleinhans F, Mazur P. 2014 Survivals of mouse oocytes approach 100% after vitrification in 3-fold diluted media and ultra-rapid warming by an IR laser pulse. Cryobiology 68:419–30 [PubMed: 24662030]
72. Jin B, Mazur P. 2015 High survival of mouse oocytes/embryos after vitrification without permeating cryoprotectants followed by ultra-rapid warming with an IR laser pulse. Scientific reports 5
73. Licht S 1974 History of Therapeutic Heat and Cold In Therapeutic Heat and Cold, 3rd Ed, ed. Lehman JF:1–34. Baltimore: Williams & Wilkins. Number of 1-34 pp.

74. Khoshnevis S, Craik NK, Diller KR. 2014 Experimental Characterization of the Domains of Coupling and Uncoupling Between Surface Temperature and Skin Blood Flow. International Journal of Transport Phenomena 13:277–301

75. Bieuzen F, Bleakley CM, Costello JT. 2013 Contrast Water Therapy and Exercise Induced Muscle Damage: A Systematic Review and Meta-analysis. PloS one 8:e62356 (1-15) [PubMed: 23626806]

76. Christmas KM, Patik JC, Khoshnevis S, Diller KR, Brothers RM. 2016 Sustained Cutaneous Vasoconstriction During and Following Cryotherapy Treatment: Role of Oxidative Stress and Rho Kinase. Microvascular Research 106:96–100 [PubMed: 27089823]

77. Khoshnevis S, Craik NK, Diller KR. 2015 Cold-induced Vasoconstriction May Persist Long After Cooling Ends: An Evaluation of Multiple Cryotherapy Units. Knee Surgery Sports Traumatology Arthroscopy 23:2475–83

78. Dewhirst MW, Abraham J, Viglianti B. 2015 Evolution of Thermal Dosimetry for Application of Hyperthermia to Treat Cancer. Advances in Heat Transfer 47:397–421

79. Jiang J, Goel R, Schmechel S, Vercellotti G, Forster C, Bischof J. 2010 Pre-conditioning Cryosurgery: Cellular and Molecular Mechanisms and Dynamics of TNF-alpha Enhanced Cryotherapy in An in vivo Prostate Cancer Model System. Cryobiology 61:280–8 [PubMed: 20940007]

80. Heller HC, Grahn DA. 2012 Enhancing Thermal Exchange in Humans and Practical Applications. Disruptive Science and Technology 1:11–9

81. Taylor NAS, Machado-Moreira DA, van den Heuel AMJ, Caldwell AN. 2014 Hands and Feet: Physiological Insulators, Radiators and Evaporators. European Journal of Applied Physiology 114:2037–60 [PubMed: 25011493]

82. Tansey Ea, Johnson CD. 2015 Recent Advances in Thermoregulation. Advances in Physiology Education 39:139–48 [PubMed: 26330029]

83. Johnson JM, Minson CT, Kellogg DL Jr. 2014 Cutaneous Vasodilator and Vasoconstrictor Mechanisms in Temperature Regulation. Comprehensive Physiology 4:33–89 [PubMed: 24692134]

84. Kurz A 2008 Physiology of Thermoregulation. Best Practice & Research Clinical Anaesthesiology 22:627–44 [PubMed: 19137807]

85. Diller KR. 2015 Therapeutic Recruitment of Thermoregulation in Humans by Selective Thermal Stimulation along the Spine. Advances in Heat Transfer 47:341–96

86. Diller KR. 2015 Heat Transfer in Health and Healing. Journal of Heat Transfer 137:103001 (1-12)

87. Goltz F, Ewald JR. 1896 Der Hund mit verkurztem Ruckenmark. Pflugers Archiv 63:362–400

88. Jessen C 2001 Temperature Regulation in Humans and Other Mammals. Berlin: Springer

89. Jessen C, McLean JA, Calvert DT, Findlay JD. 1972 Balanced and Unblanced Temperature Signals Generated in the Spinal Cord of the Ox. American Journal of Physiology 222:1343–7 [PubMed: 5030191]

90. Jessen C, Felde D, Volk P, Kuhnen G. 1990 Effects of Spinal Cord Temperature on the Generation and Transmission of Temperature Signals in the Goat. Pflugers Archiv 416:428–33 [PubMed: 2169044]

91. Hales JRS, Fawcett AA, Bennett JW, Needham AD. 1978 Thermal Control of Blood Flow Through Capillaries and Arteriovenous Anastomoses in Skin of Sheep. Pflugers Archiv 378:55–63 [PubMed: 569825]

92. Hales JRS, Fawcett AA, Bennett JW. 1975 Differential Influences of CNS and Superficial Body Temperatures on the Partition of Cuteneous Blood Flow between Capillaries and Arteriovenous Anastomoses (AVA's). Pflugers Archiv 361:105–6 [PubMed: 1239737]

93. Jessen C, Mayer ET. 1971 Spinal Cord and Hypothalamus as Core Sensors of Temperature in the Conscious Dog. I. Equivalence of Responses. Pflugers Archiv 34:189–204

94. Jessen C, Ludwig O. 1971 Spinal Cord and Hypothalamus as Core Sensors of Temperature in the Conscious Dog. II. Addition of Signals. Pflugers Archiv 324:205–16 [PubMed: 5102606]

95. Jessen C, Simon E. 1971 Spinal Cord and Hypothalamus as Core Sensors of Temperature in the Conscious Dog. III. Identity of Functions. Pflugers Archiv 324:217–26 [PubMed: 5102607]

96. Carlisle HJ, Ingram DL. 1973 The Influence of Body Core Temperature and Peripheral Temperatures on Oxygen Consumption in the Pig. Journal of Physiology 231:341–52 [PubMed: 4720936]

97. Meurer K-A, Jessen C, Iriki M. 1967 Kaltezittern wahrend isolierter Kuhlung des Ruckenmarkes nach Durchschneidung der Hinterwurzeln. Pflugers Archiv 293:236–55

98. Wunnenberg W, Bruck K. 1970 Studies on the ascending Pathways from the Thermosensitive Region of the Spinal Cord. Pflugers Archiv 321:233–41 [PubMed: 4921904]

99. Hales JRS, Iriki M, K. T, Kozawa E. 1978 Thermally-Induced Cutaneous Sympathetic Activity Related to Blood Flow Through Capillaries and Arteriovenous Anastomoses. Pflugers Archiv 375:17–24 [PubMed: 567339]

100. Chai CY, Lin MT. 1972 Effects of Heating and Cooling the Spihnal Cord and Medulla Oblongata on Thermoregulation in Monkeys. Journal of Physiology 225:297–308 [PubMed: 4627523]

101. Kosaka M, Simon E. 1968 Kaltetremor wach, chronisch spinalisierter Kaninchen im Vergleich zum Kaltezittern intaker Tiere. Pflugers Archiv 302:333–56 [PubMed: 5246534]

102. Guieu JD, Hardy JD. 1970 Effects of Preoptic and Spinal Cord Temperature in Control of Thermal Polypnea. Journal of Applied Physiology 28:540–2 [PubMed: 5437448]

103. Rautenberg W, Necker R, May B. 1972 Thermoregulatory Responses of the Pigeon to Changes of the Brain and the Sprinal Cord. Pflugers Archiv 338:31–42 [PubMed: 4675231]

104. Hammel HT, Maggert J, Kaul R. 1976 Effects of Altering Spinal Cord Temperature on Temperature REgulation in the Adelie Penguin, Pygoscelis Adeliae. Pflugers Archiv 362:1–6 [PubMed: 943774]

105. Helfmann W, Jannes P, Jessen C. 1981 Total Body Thermosensitivity and Its Spinal and Supraspinal Fractions in the Conscious Goose. Pflugers Archiv 391:60–7 [PubMed: 7279602]

106. Andresson B, Ekman L, Gale CC, Sundsten JW. 1963 Control of Thyrotrophic Hormone (TSH) Secretion by the "Heat Loss Center". Acta Physiologica Scandanavia 59:12–33

107. Hensel H 1973 Neural Processes in Thermoregulation. Physiological Reviews 53:948–1017 [PubMed: 4355518]

108. Sessler DI. 2013 The Thermoregulation Story. Anesthesiology 118:181–6 [PubMed: 23221865]

109. Grahn DA, Brock-Utne JG, Watenpaugh DE, Heller HC. 1998 Recovery from Mild Hypothermia Can Be Accelerated by Mechanically Distending Blood Vessels in the Hand. Journal of Applied Physiology 85:1643–8 [PubMed: 9804564]

110. Grahn DA, Dillon JL, Heller HC. 2009 Heat Loss Through the Glabrous Skin Surfaces of Heavily Insulated, Heat-Stressed Individuals. Journal of Biomechanical Engineering 131:071005: 1-7 [PubMed: 19640130]

111. Grahn DA, Murray JV, Heller HC. 2008 Cooling via One Hand Improves Physical Performance in Heat-Sensitive Individuals with Multiple Sclerosis: a Preliminary Study. BMC neurology 8:1–8 [PubMed: 18211709]

112. Kurz A, Xiong J, Sessler DI, Dechert M, Noyes K, Belani K. 1995 Desflurane Reduces the Gain of Thermoregulatory Arteriovenous Shunt Vasoconstriction in Humans. Anesthesiology 83:1212–9 [PubMed: 8533914]

113. Kurz A, Go JC, Sessler DI, Kaer K, Larson MD, Bjorkstein AR. 1995 Alfentanil Slightly Increases the Sweating Threshhold and Markedly Reduces the Vasoconstriction and Shivering Thresholds. Anesthesiology 83:295–9

114. Kurz A, Ikeda T, Sessler DI, Larson MD, Bjorkstein AR, et al. 1997 Meperidine Decreases the Shivering Threshold Twice as Much as the Vasoconstriction Threshold. Anesthesiology 86:1046–54 [PubMed: 9158353]

115. Matsukawa T, Kurz A, Sessler DI, Bjorkstein AR, Merrifield B, Cheng C. 1995 Propofol Linearly Reduces the Vasoconstriction and Shivering Thresholds. Anesthesiology 82:1169–80 [PubMed: 7741292]

116. Matsukawa T, Kurz A, Sessler DI, Bjorksten AR, Merrifield B, Cheng C. 1995 Propofol Linearly Reduces the Vasoconstriction and Shivering Thresholds. Anesthesiology 82:1169–80 [PubMed: 7741292]

117. Xiong J, Kurz A, Sessler DI, Plattner O, Christensen R, et al. 1996 Isoflurance Produces Marked and Nonlinear Decreases in the Vasoconstriction and Shivering Thresholds. Anesthesiology 85:240–45 [PubMed: 8712437]
118. Reynolds L, Beckmann J, Kurz A. 2008 Perioperative Complications of Hypothermia. Best Practice & Research Clinical Anaesthesiology 22:645–57 [PubMed: 19137808]
119. Rajagopalan S, Mascha E, Na J, Sessler DI. 2008 The Effects of Mild Perioperative Hypothermia on Blood Loss and Transfusion Requirement. Anesthesiology 108:71–7 [PubMed: 18156884]
120. Flores-Maldonado A, Medina-Escobedo CE, Rios-Rodriguez HMG, Fernandez-Dominguez R. 2001 Mild Perioperative Hypothermia and the Risk of Wound Infection. Archives of Medical Research 32:227–31 [PubMed: 11395189]
121. Lenhardt R, Marker E, Goli V, Tschernich H, Kurz A, et al. 1997 Mild Intraoperative Hypothermia Prolongs Postanesthetic Recovery. Anesthesiology 87:1318–23 [PubMed: 9416715]
122. Kurz A, Sessler DI, Lenhardt R. 1996 Perioperative Normothermia to Reduce the Incidence of Surgical-wound Infection and Shorten Hospitalization. New England Journal of Medicine 334:1209–15 [PubMed: 8606715]
123. Frank SM, Fleisher LA, Breslow MJ. 1997 Perioperative Maintenance of Normothermia Reduces the Incidence of Morbid Cardiac Events: A Randomized Clinical Trial. Journal of the American Medical Association 277:1127–34 [PubMed: 9087467]
124. Giesbrecht GG, Cucharme MB, McGuire JP. 1994 Comparison of Forced-air Patient Warming Systems for Preioperative Use. Anesthesiology 80:671–9 [PubMed: 8141463]
125. Taguchi A, Ratnaraj J, Kabon B, Sharma N, Lenhardt R, et al. 2004 Effects of a Circulating-water Garment and Forced-air Warming on Body Heat Content and Core Temperature. Anesthesiology 100:1058–64 [PubMed: 15114200]
126. Sandoval MF, Mongan PD, Dayton MR, Hogan CA. 2017 Safety and Efficacy of Resistive Polymer Versus Forced Air Warming in Total Joint Surgery. Patient Safety in Surgery 11:11:1-6 [PubMed: 28416968]
127. Negishi C, Hasegawa K, Mukai S, Nakagawa F, Ozaki M, Sessler DI. 2003 Resistive-Heating and Forced-Air Warming Are Comparably Effective. Anesthesia & Analgesia:1683–7 [PubMed: 12760996]
128. Ruetzler K, Kovaci B, Guloglu E, Kabon B, Fleischmann E, et al. 2011 Forced-Air and a Novel Patient-Warming System (vitalHEAT vH2) Comparably Maintain Normothermia During Open Abdominal Surgery. Anesthesia and analgesia 112:608–14 [PubMed: 20841410]
129. Sun A, Honar H, Sessler DI, Dalton JE, Yang D, et al. 2015 Intraoperatiev Core Temperature Patterns, Transfusion Requirement, and Hospital Duration in Patients Warmed with Forced Air. Anesthesiology 122:276–85 [PubMed: 25603202]
130. Legg AJ, Hamer AJ. 2013 Forced-air Patient Warming Blankets Disrupt Unidirectional Airflow. The Bone & Joint Journal 95-B:407–10 [PubMed: 23450029]
131. Weissman C, Murray WB. 2013 It's not just another room. Anesthesia and analgesia 117:287–9 [PubMed: 23881369]
132. Wood AM, Moss C, Keenan A, Reed MR, Leaper DJ. 2014 Infection Control Hazards Associated with the Use of Forced-air Warming in Operating Theatres. The Journal of hospital infection 88:132–40 [PubMed: 25237035]
133. Belani KG, Albrecht M, McGovern PD, Reed M, Nachtsheim C. 2013 Patient Warming Excess Heat: the Effects on Orthopedic Operating Room Ventilation Performance. Anesthia and Analgesia 117:406–11
134. Taylor NAS, Caldwell JN, van den Heuvel AMJ, Patterson MJ. 2008 To Cool, but Not Too Cool: That is the Question--ImmersionCooling for Hyperthermia. Medicine and science in sports and exercise 40:1962–9 [PubMed: 18845977]
135. Van Someren EJW. 2000 More Than a Marker: Interaction Between the Circadian Regulation of Temperature and Sleep, Age-Related Changes, and Treatment Possibilities. Chronobiology International 17:313–54 [PubMed: 10841209]
136. Krauchi K 2007 The Human Sleep-Wake Cycle Reconsidered from a Thermoregulatory Point of View. Physiology & behavior 90:236–45 [PubMed: 17049364]

137. Gilbert SS, Burgess HJ, Kennaway DJ, Dawson D. 2000 Attenuation of Sleep Propensity, Core Hypothermia, and Peripheral Heat Loss After Temazepam Tolerance. American Jounral of Physiology, Regulaory Integrative Comparative Physiology 279:R1980–R7

138. Krauchi K, Knoblauch R, Wirz-Justice A, Cajochen C. 2006 Challenging the Sleep Homeostat Does Not Influence the Thermoregulatory System in Men: Evidence From a Nap vs. Sleep-Deprivation Study. American Journal of Physiology: Regulatory, Integrative and Comparative Physiology 290:R1052–R61

139. Krauchi K, Werth E, Wirz-Justice A. 1999 Warm Feet Promote the Rapid Onset of Sleep. Nature 401:36–7 [PubMed: 10485703]

140. Pache M, Kräuchi K, Cajochen C, Wirz-Justice A, Dubler B, et al. 2001 Cold Feet and Prolonged Sleep-Onset Latency in Vasospastic Syndrome. The Lancet 358:125–6

141. Gradisar M, Lack L. 2004 Relationships Between the Circadian Rhythms of FingerTemperature, Core Temperature, Sleep Latency, and Subjective Sleepiness. Journal of biological rhythms 19:157–63 [PubMed: 15038855]

142. Smolensky MH, Hermida RC, Castriotta RJ, Portaluppi F. 2007 Role of Sleep-Wake Cycle on Blood Pressure Circadian Rhythms and Hypertension. Sleep medicine 8:668–80 [PubMed: 17383936]

143. Hermida RC, Ayala DE, Fernandez J, Mojon A. 2013 Sleep-Time Blood Pressure: Prognostic Value and Relevance as a Therapeutic Target for Cardiovascular Risk Reduction. Chronobiology International 30:68–86 [PubMed: 23181592]

144. Hermida RC, Ayala DE, Mojon A, Fernandez JR. 2013 Blunted Sleep-Time Relative Blood Pressure Decline Increases Cardiovascular Risk Independent of Blood Pressure Level--the "Normotensive Non-Dipper" Paradox. Chronobiology International 30:87–98 [PubMed: 23039824]

145. Foundation NS. 2005 2005 National Sleep Foundation Poll

146. Leger D, Bayon V, Ohayon MM, Philip P, Ement P, et al. 2014 Insomnia and Accidents: Cross-Sectional Study (EQUINOX) on Sleep-Related Home, Work and Car Accidents in 5293 Subjects with Insomnia From 10 Countries. Journal of sleep research 23:143–52 [PubMed: 24237855]

147. Smolensky MH, Di Milia L, Ohayon MM, Philip P. 2011 Sleep Disorders, Medical Conditions, and Road Accident Risk. Accident; analysis and prevention 43:533–48 [PubMed: 21130215]

148. Lack LC, Gradisar M, Van Someren EJ, Wright HR, Lushington K. 2008 The Relationship Between Insomnia and Body Temperatures. Sleep medicine reviews 12:307–17 [PubMed: 18603220]

149. Krauchi K 2007 The Thermophysiological Cascade Leading to Sleep Initiation in Relation to Phase of Entrainment. Sleep Med Rev 11:439–51 [PubMed: 17764994]

150. Krauchi K, Cajochen C, Werth E, Wirz-Justice A. 2000 Functional Link Between Distal Vasodilation and Sleep-onset Latency? American Journal of Physiology Regulatory Integrative Camparative Physiology 278:R741–R8

151. Cheng C, Matsukawa T, Sessler DI, Ozaki M, Kurz A, et al. 1995 Increasing Mean Skin Temperature Linearly Reduces the Core-temperature Thresholdsfor Vasoconstriction and Shivering in Humans. Anesthesiology 82:1160–8 [PubMed: 7741291]

152. Lenhardt R, Greif R, Sessler DI, Laciny S, Rajek A, Bastanmehr H. 1999 Relative Contribution of Skin and Core Temperatures to Vasconstriction and Shivering Thresholds during Isoflurane Anesthesia. Anesthesiology 91:422–9 [PubMed: 10443605]

SIDEBARS

Selective Thermal Stimulation. It has long been recognized that a primary site for thermoregulatory thermostat control is resident in the brain (preoptic anterior hypothalamus). However, it has now been documented that parallel thermostat structures exist peripheral to the brain, most prominently along the spinal cord. This peripheral location provides an opportunity to apply safe noninvasive thermal stimulation to manipulate thermoregulatory function to therapeutic or prophylactic advantage for a number of important physiological applications. STS offers an approach to orchestrating thermoregulatory function that is both effective and safe since uses gentle thermal stimulation methods to cooperatively conscript the body's natural mechanisms for moving heat between the core and periphery. The result is that devices can be used that combine simple componentry and function with sophisticated physiological principles of operation.

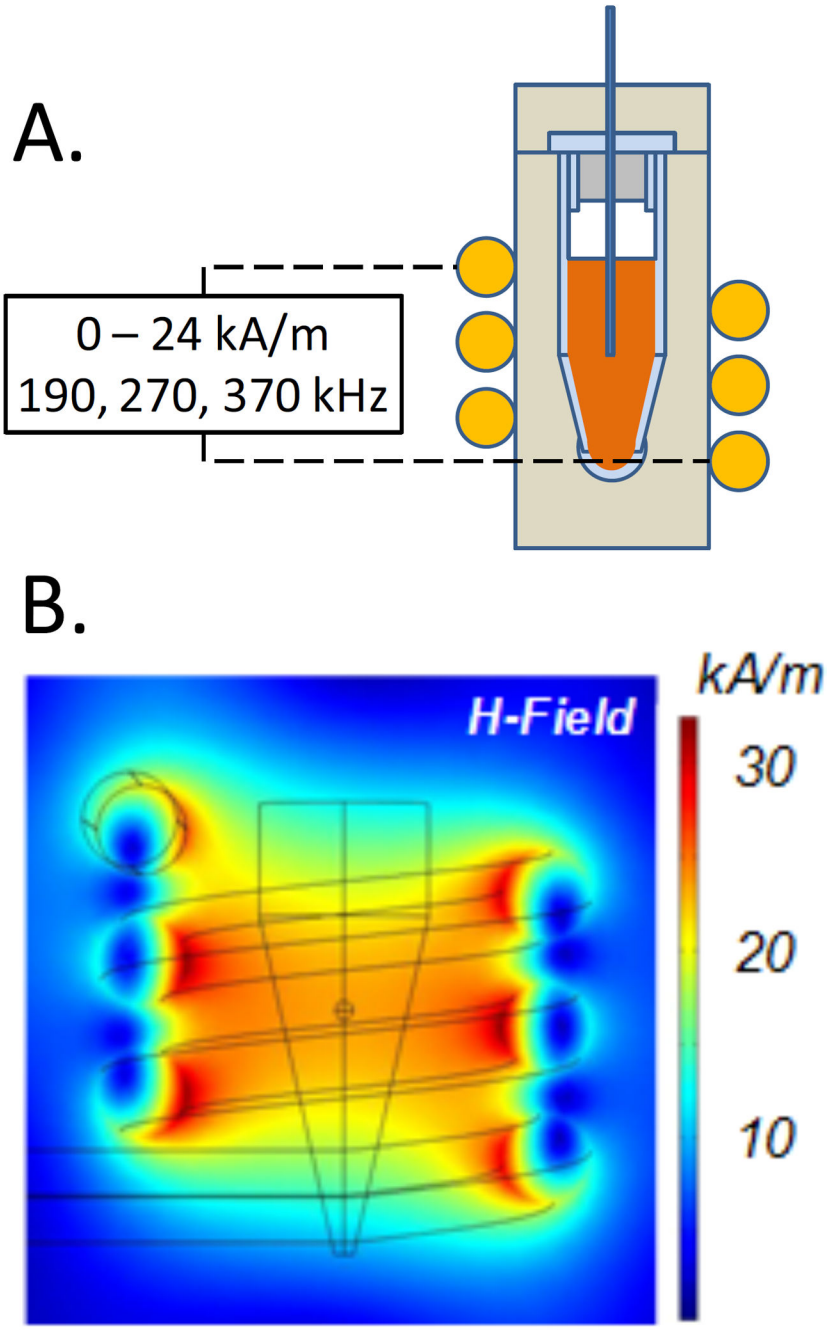

Figure 1.
SAR and ΔT measurements during iron oxide (IO) nanoparticle heating. (A) typical field strength and frequencies used in an inductive RF coil to heat solutions and tissues loaded with IO nanoparticles. (B) COMSOL model of the field strength within the RF coils used to heat the IO nanoparticle laden systems (Modified from (26)).

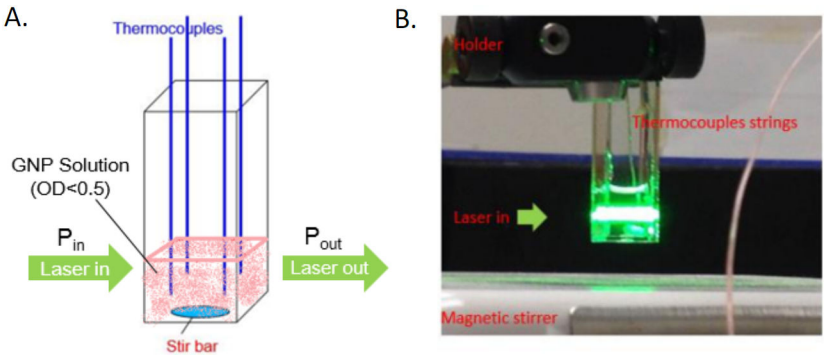

Figure 2.

Photothermal heating experimental setup to determine SAR and Cabs. (A) Schematic and image of experimental setup; (B) heating experiment where P_{in} and P_{out} is measured to establish gold nanoparticle SAR. The SAR is calibrated to a resistor dissipating a known amount of heat. Figure modified and reproduced from (46) with permission.

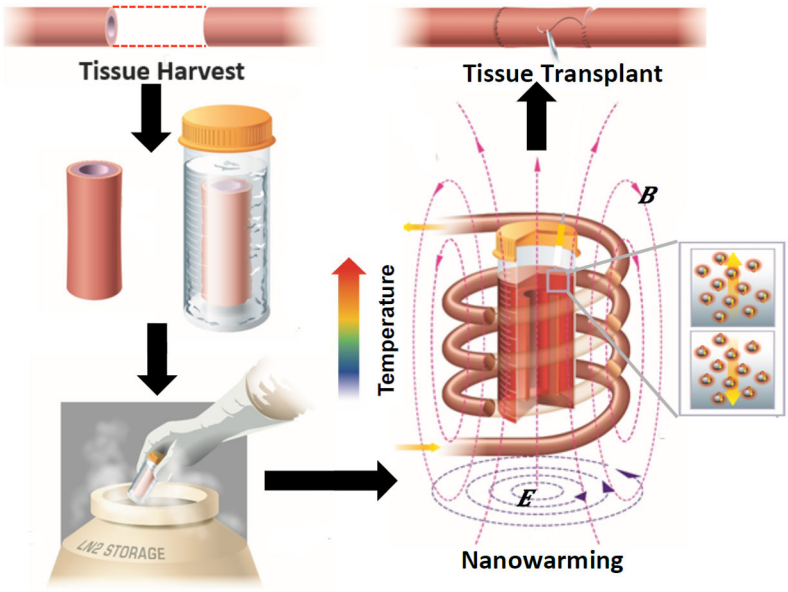

Figure 3.

Nanowarming for Regenerative Medicine. Schematic of tissue harvest followed by cryoprotective agent loading and cooling into gaseous nitrogen. After storage the IO nanoparticles loaded into the system are activated in a radiofrequency field to quickly and uniformly warm the system to avoid devitrification (i.e. crystallization) and cracking. This allows for high viability and function which can eventually be used in transplantation. Modified and reproduced with permission from (14).

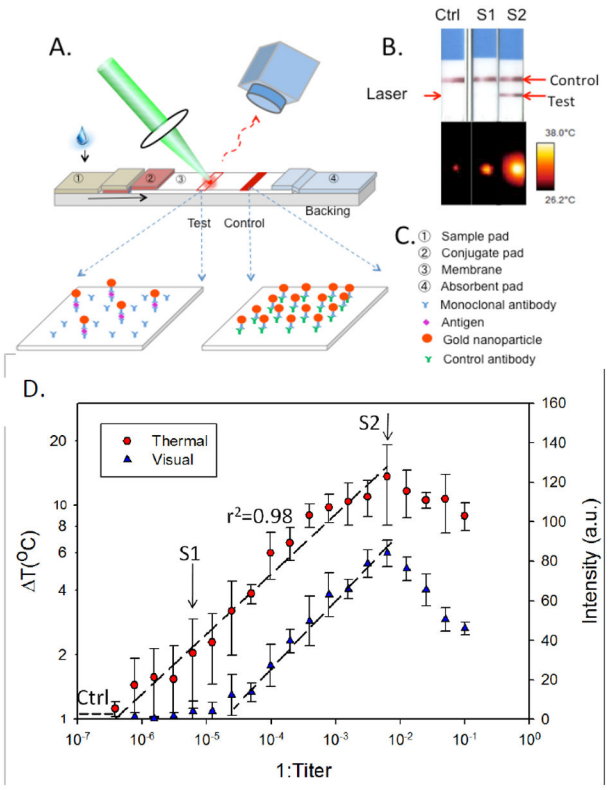

Figure 4.

Thermal contrast for improved lateral flow assay diagnostics: (A) Schematic of the Thermal Contrast approach; (B) visual vs. thermal results for negative control, visually negative but thermally positive (S1) and visually positive (S2) LFAs. (C) LFA design components; (D) thermal vs. visual contrast of a dilution study on Cryptococcus infected patient blood demonstrated 32 fold improvement. Reproduced with permission from (15).

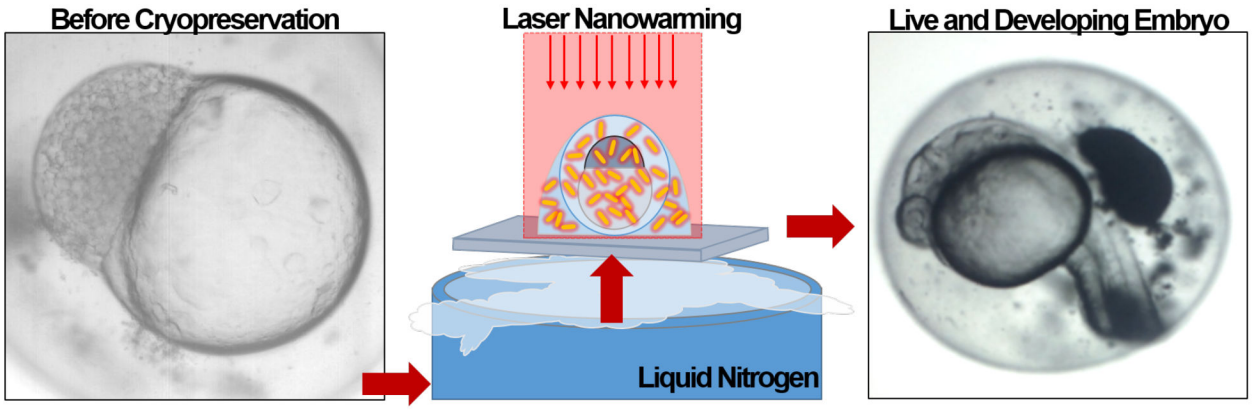

Figure 5.

Gold laser nanowarming for improved zebrafish embryo cryopreservation. Here gold nanorods and cryoprotective agents are micro-injected into a zebrafish embryo prior to cryogenic stabilization. Warming is achieved by plasmonically coupling to the gold nanorods with a laser for fast and uniform warming to avoid devitrification and cracking. The zebrafish can then continue to grow and mature. Reproduced with permission from (16).

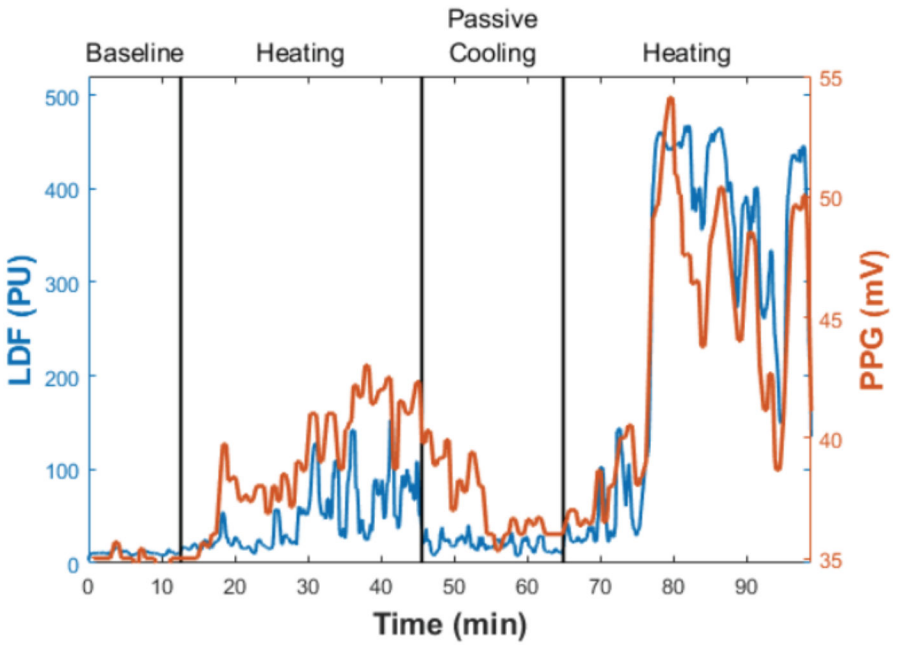

Figure 6.

Plot of blood flow in the finger pad during an STS trial. Perfusion is plotted on the vertical axis as parallel laser Doppler flowmeter (LDF) and photo plethysmography (PPG) outputs in arbitrary units. STS was applied by heating on the skin surface at the cervical spine at a temperature of 40°C. Baseline data shows a high level of vasoconstriction. STS was active from 13 to 43 min, followed by 20 minutes of passive cooling, and then a second STS episode starting at 63 min.

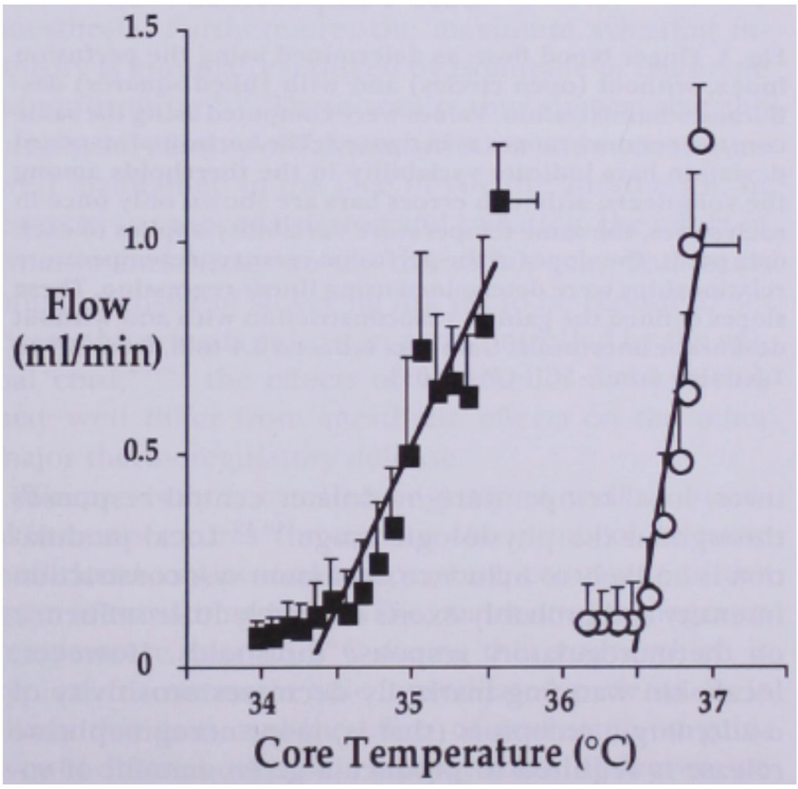

Figure 7.

Kurz and Sessler experiment to measure the effect of anesthesia (Desflurane) on depression of threshold core temperature for initiation of vasoconstriction of AVAs during cooling from a thermoneutral state (112). Mean skin temperature was held constant during venous infusion of cold fluid to drop core temperature at 1.5°C/hr. Separate trials were conducted on two days with and without (control) anesthesia. The anesthesia dropped the vasoconstriction threshold temperature by 1.2°C and reduced the gain by a factor of about 3.

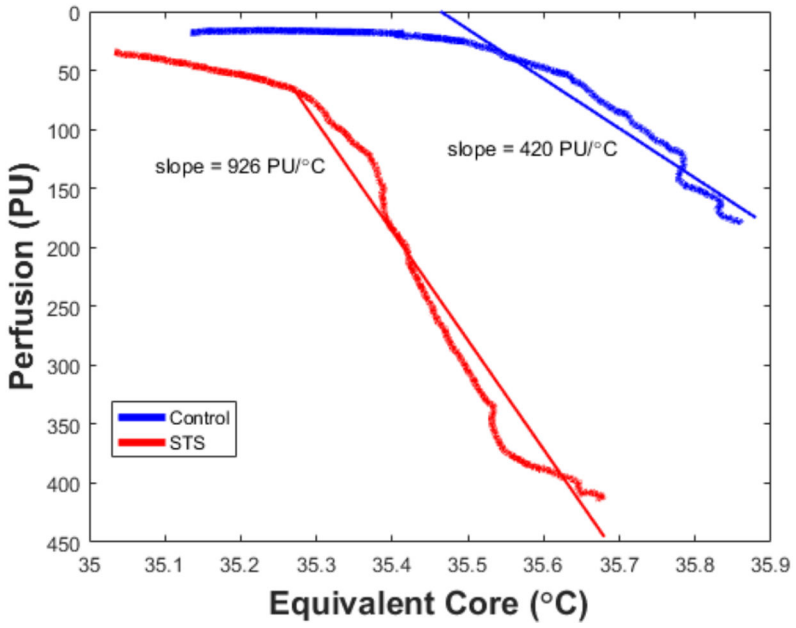

Figure 8.

A similar experiment conducted with STS rather than anesthesia. Equivalent core temperature was calculated as the weighted average of actual core (80%) and mean skin (20%) temperatures (151; 152) during cooling from a thermoneutral state of full AVA vasoconstriction achieved by adjusting circulating water temperature in a full body suit. Mean skin temperature was dropped by reducing temperature of water circulated through the suit. STS was applied continuously starting at the thermoneutral state, achieving a higher GSBF prior to cooling. STS reduced the vasoconstriction threshold temperature by about 0.5°C, but increased the gain by a little over 2.

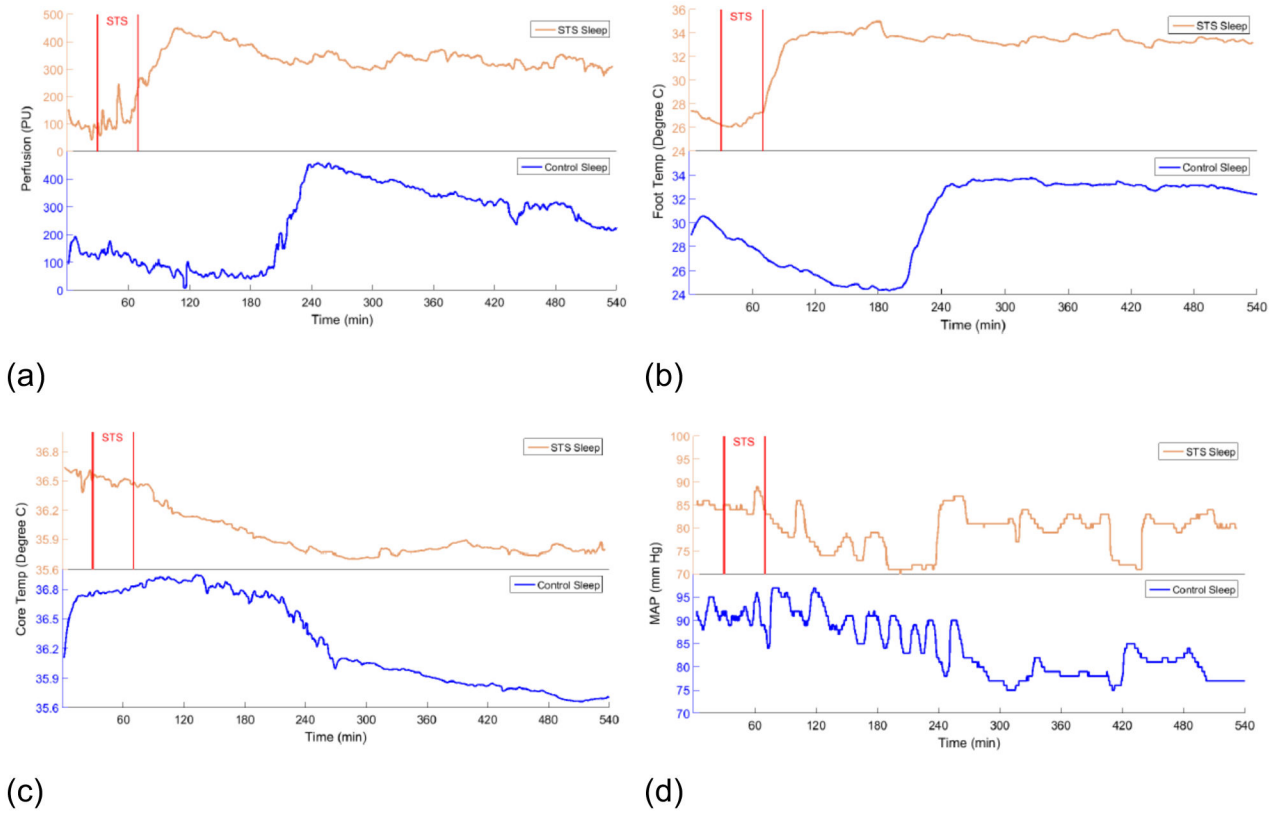

Figure 9.

Overnight physiological data measured on a subject who slept one night without using STS (lower blue plots) and one night with STS applied for 30 minutes at the time of going to bed (upper orange plots). The start and finish of STS are denoted by the vertical lines. (a) Blood flow to glabrous skin of foot measured from an initial 20 min baseline period. (b) Temperature on the foot sole. (c) Core temperature measured with a sublingual probe. (d) Mean arterial blood pressure.